

**Lg WAVE SIMULATIONS IN HETEROGENEOUS CRUSTS  
WITH IRREGULAR TOPOGRAPHY  
USING HALF-SPACE SCREEN PROPAGATORS**

R.S. Wu, X.B. Xie and X.Y. Wu, Institute of Tectonics, University of California, Santa Cruz

Sponsored by U.S. Department of Defense  
Defense Threat Reduction Agency  
Contract No.: DSWA01-97-1-0004

**ABSTRACT**

This study is aimed at development and application of a new wave propagation and modeling method for regional waves in heterogeneous crustal waveguides using one-way wave approximation. The half-space GSP (generalized screen propagator) has taken the free surface into the formulation and adopts a fast dual-domain implementation. The method is several orders of magnitude faster than finite-difference methods with a similar accuracy for certain problems. It has been used for the simulation of wave propagation for high-frequency waves (1 - 20 Hz) to a regional distance (greater than 1000 km).

In this year we further developed the method in three aspects. First, we extend the GSP method to treat irregular surface topography by incorporating a coordinate transform into the method. Both conformal and non-conformal transformations have been introduced and their relative merits and accuracies have been discussed. Comparison with boundary element integration method showed that the extended method works well for mild topographies. Accuracy improvement for rough topography is still an ongoing research. Second, we developed a hybrid method which couples the fast screen propagator method with a modified boundary element method to treat the problems with severe rough topography. Finally, numerical simulations have been conducted for various crustal waveguide structures, including both deterministic structures and small-scale random heterogeneities and random rough surfaces. Influence of random heterogeneities and rough surfaces on Lg amplitude attenuation and Lg coda formation are shown to be significant. In collaboration with T. Lay, we have investigated the frequency- dependent Lg attenuation and blockage both observationally and numerically. The comparison between the observation and numerical simulations reveals many interesting phenomena and needs more thorough investigation.

**Key Words:** seismic wave propagation, crustal structure, discrimination

## **INTRODUCTION**

Crustal guided wave Lg provides valuable information for nuclear test monitoring and yield estimation. Lg energy mainly propagates in the crustal wave guide and the uppermost mantle. The low velocity crust provides an ideal channel for Lg propagation. On the other hand, many crustal characteristics, both deterministic structures (e.g., crustal necking, thickening) and stochastic characteristics (e.g., random volume heterogeneities in the crust, random fluctuations at free surface and Moho discontinuity) affect the propagation of the Lg wave. To isolate path effects from the source parameters, a clear understanding of these mechanisms and how they affect the Lg attenuation is crucial. In these investigations, numerical methods for simulating Lg wave propagation based on realistic deterministic and/or stochastic models are often very useful.

The existing methods for calculating synthetic regional phases can be roughly categorized into three groups. (1). Wavenumber integration method (e.g., Bouchon 1981, Campillo 1990). This method originally handles only laterally homogeneous media and is incapable of handling complex 3D structures and heterogeneities. Later developments (e.g., Bouchon et al. 1989; Chen, 1990, 1995) extend the capability of the method to handle large-scale lateral variations, but volume heterogeneities are still excluded. (2). Normal mode approach (e.g. Wang and Hermann 1988). This method works well for layered media, and later development of coupled mode theory (Kennett, 1984) enables it to handle slightly lateral variations, but is limited in its validity for strong lateral variations. (3). Fully discretized numerical methods, for example finite-difference method (Xie and Lay, 1994; Jih, 1996; Hestholm and Ruud, 1994, 1998) and boundary element method (e.g., Fu and Wu, 1999). In principle, finite-difference method can deal with arbitrarily heterogeneous media including both volume heterogeneities and rough free surfaces. The boundary element method can handle arbitrary free surfaces and interfaces but is not very powerful in dealing with volume heterogeneities. However, under realistic conditions, i.e., complex waveguide with volume heterogeneities and free-surface/interface fluctuations, high frequency and long propagation distances, the ability of all the above mentioned methods is very limited. Yet under over simplified velocity models, lower frequencies and shorter propagation ranges, many practical issues associated with the regional phase propagation can not be properly investigated.

In the crustal waveguide environment, major wave energy is carried by forward propagating waves, including forward scattered waves, therefore neglecting backscattered waves in the propagation will not change the main features of regional waves in most cases. Based on this concept, a generalized screen propagator method (GSP) based on the one-way wave equation has been developed by Wu (1994), Wu, Jin and Xie (1999a) and has been successfully used to simulate SH Lg waves in the complex crustal waveguide and investigate the energy partitioning of Lg waves (Wu, Jin and Xie, 1999b). This method neglects backscattered waves, but correctly handles all the forward multiple-scattering effects, e.g., focusing/defocusing, diffraction, interference, etc. The method is two to three orders of magnitude faster than the finite-difference method for medium sized problems.

In this paper we further extend the GSP method to treat irregular surface topography by incorporating coordinate transforms into the method. Both conformal and non-conformal transforms have been introduced and their relative merits and accuracies have been discussed. Comparison with other exact methods, such as the boundary element integration method, showed that the extended method works well for mild to moderate topographies. Numerical simulations have been conducted for various crustal waveguide structures, including both deterministic structures and random rough surfaces.

### **CONFORMAL COORDINATE TRANSFORM FOR GSP**

General wide-angle formulation. For a 2D SH problem and under the perturbation theory, the frequency domain wave equation for the y-component of displacement field can be written as (Wu, et al. 1999a)

$$(\nabla^2 + k^2)u(\mathbf{r}) = -k^2 F(\mathbf{r})u(\mathbf{r}) \quad (1)$$

where  $k = \omega/v$  is the wavenumber in the background medium,  $v$  is the background S wave velocity defined

by  $v = (\mu_0 / \rho_0)^{1/2}$ , and  $\mu_0$  and  $\rho_0$  are background values of  $\mu$  and  $\rho$ . In the right hand side of (1),  $F(r)$  is a perturbation operator

$$F(r) = \epsilon_p(r) + \frac{1}{k^2} \nabla^2 \epsilon_\mu \quad (2)$$

with  $\epsilon_p(r) = (\rho(r) / \rho_0) - 1$  and  $\epsilon_\mu(r) = \mu(r) / \mu_0 - 1$ , where  $\rho(r)$  and  $\mu(r)$  are perturbations of  $\rho$  and  $\mu$ . Equation (1) is a scalar Helmholtz equation. For flat free surfaces, Wu et al. (1999a) derived a half-space GSP solution for Lg wave propagation. In the case of irregular topography, the global mirror symmetry for the problem no longer

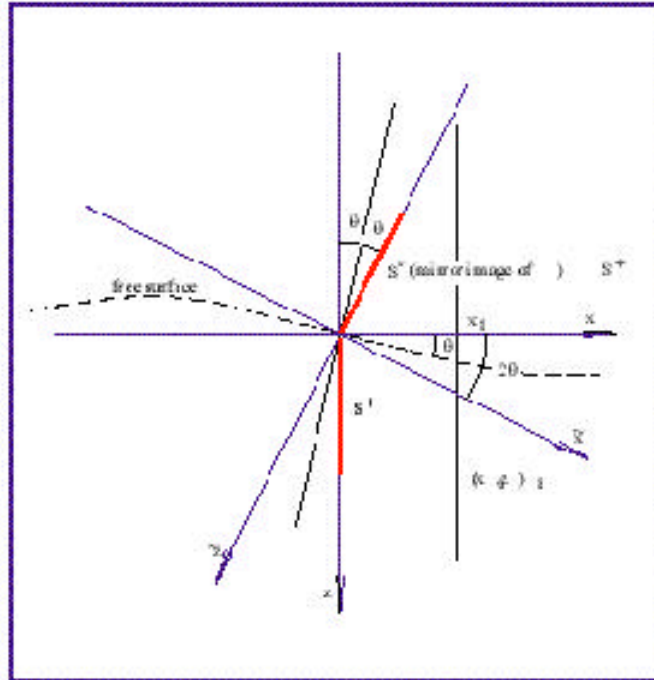


Figure 1: Geometry of the coordinate transform.

exists. However, if a first order approximation (local plane-surface approximation) for the topography is taken, we can modify the mirror image method to a local mirror image method and apply the corresponding coordinate transform to obtain a GSP solution for this case.

Fig. 1 shows the geometry of the derivation. Assume  $u_0^+$  is the incident field on  $S^+$ , then  $u_0^-$  on  $S^-$  is also known as the mirror image of  $u_0^+$  about the local plane surface. The total wavefield composed of  $S^+$  and  $S^-$  is the sum of the primary field which propagates in the homogeneous background medium and the scattered field which is generated by the local heterogeneities in the thin-slab. The effects of the heterogeneities and the topography can be calculated separately for each step in the GSP method. The effect of the slant free-surface can be incorporated into the propagation integral. Assume  $u_t(x, z)$  is the total field including the scattering effect of the volume heterogeneities. The field  $u(x_1, z_1)$  in front of the integral surface can be calculated by the Kirchhoff integral

$$\begin{aligned} u(x_1, z_1) &= \int_S ds \left\{ g(x, z; x_1, z_1) \frac{\partial u_t(x, z)}{\partial n} - \frac{\partial g(x, z; x_1, z_1)}{\partial n} u_t(x, z) \right\} \\ &= \int_{S^-} ds \{ \dots \} + \int_{S^+} ds \{ \dots \} \end{aligned} \quad (3)$$

where  $g(\cdot)$  is the Green's function for the full space with homogeneous velocity distribution,  $S$  is the integration surface and  $S^+$  and  $S^-$  are the lower and upper half surfaces, respectively. The Rayleigh integral can be used to replace the Kirchhoff integral for each half surface integral. For the lower half-space the contribution of  $S^+$  is

$$\begin{aligned} u_t^+(x_1, z_1) &= -2 \int_0^{\infty} dz u_t^+(x, z) \frac{\partial g(x, z; x_1, z_1)}{\partial n} \\ &= \frac{1}{2\pi} \int dK_T e^{iK_T z_1} u_t^+(x_1, K_T) \end{aligned} \quad (4)$$

where

$$u_t^+(x_1, K_T) = e^{i\gamma(x_1 - x)} \int_0^{\infty} dz u_t^+(x, z) e^{-iK_T z} \quad (5)$$

Here  $u_t^+(x, z)$  is the total field equal to the sum of incident field  $u_0^+(x, z)$  and the scattered field  $U^+(x, z)$  caused by the heterogeneities within the slab between  $x$  and  $x_1$  (see Wu, 1994; Wu et al., 1999a). If we put the slab entrance at  $x = x'$  and the field on the screen  $S^+$  at the entrance as  $u_t^+(x', z')$ , then

$$u_t^+(x', z') = u_0^+(x', z') + U^+(x', z') \quad (6)$$

$$\begin{aligned} U^+(x', z') &= k^2 \int_{x'}^{x_1} dx e^{-i\gamma(x_1 - x)} \int_0^{\infty} dz \{g(x_1, z_1; x, z) \varepsilon_\rho(x, z) u_0(x, z) \\ &\quad - \frac{1}{k_2} g(x_1, z_1; x, z) \cdot \varepsilon_\mu(x, z) u_0(x, z)\} \end{aligned} \quad (7)$$

For the bent upper half screen, we perform a coordinate transform by clockwise rotation of  $2\theta$  to a new coordinate system  $(\tilde{x}, \tilde{z})$ . Taking the downward direction as positive  $z$ -direction, and the rotation angle from  $x$  to  $z$  as positive, the relation connecting the two systems is

$$\tilde{x} = x \cos 2\theta + z \sin 2\theta \quad (8)$$

$$\tilde{z} = -x \sin 2\theta + z \cos 2\theta \quad (9)$$

In the new system, the surface  $S^-$  is parallel to the  $i$ -axis, so that

$$u_t^-(\tilde{x}_1, \tilde{K}_T) = e^{i\tilde{\gamma}(\tilde{x}_1 - \tilde{x}')} \int_{-\infty}^0 d\tilde{z}' u_t^-(\tilde{x}', \tilde{z}') e^{-i\tilde{K}_T \tilde{z}'} \quad (10)$$

where  $u_t^-(\tilde{x}', -\tilde{z}') = u_t^+(x', z')$  The field in the space domain can be obtained by synthesizing the contributions from all the plane waves

$$u_t^-(\tilde{x}_1, \tilde{z}) = \int d\tilde{K}_T e^{i\tilde{\gamma}(\tilde{x}_1 - \tilde{x}')} e^{i\tilde{K}_T \tilde{z}} u_t^-(\tilde{x}', \tilde{K}_T) \quad (11)$$

where

$$u_t^-(\tilde{x}', \tilde{K}_T) = \int_{-\infty}^0 d\tilde{z}' u_t^-(\tilde{x}', \tilde{z}') e^{-i\tilde{K}_T \tilde{z}'} \quad (12)$$

Transformed back to the original coordinate system, resulting in

$$u_t^-(x_1, z_1) = \int dK_T \exp \left\{ i \left[ (\tilde{\gamma} \cos 2\theta - K_T \sin 2\theta)(x_1 - x') + (\tilde{\gamma} \sin 2\theta + K_T \cos 2\theta)z_1 \right] \right\} u_t^-(x', K_T) \quad (13)$$

We can see that in the original coordinate system, the effective transversal and propagating wavenumbers are

$$\begin{cases} \gamma = \tilde{\gamma} \cos 2\theta - K_T \sin 2\theta \\ K_T = \tilde{\gamma} \sin 2\theta + K_T \cos 2\theta \end{cases} \quad (14)$$

If we transform the  $(\tilde{k}_T, \tilde{\gamma})$  system into  $(K_T, \gamma)$ ,

$$u_t^-(x_1, z_1) = \int dK_T u_t^-(x', K_T \cos 2\theta - \gamma \sin 2\theta) e^{i\gamma(z_1 - x')} e^{iK_T z_1} \quad (15)$$

The total field is a summation of the contributions from both  $u_t^+(x_1, z_1)$  and  $u_t^-(x_1, z_1)$

$$u(x_1, z_1) = \int dK_T e^{i\gamma(z_1 - x')} e^{iK_T z_1} [u_t^+(x', K_T) + u_t^-(x', K_T \cos 2\theta - \gamma \sin 2\theta)] \quad (16)$$

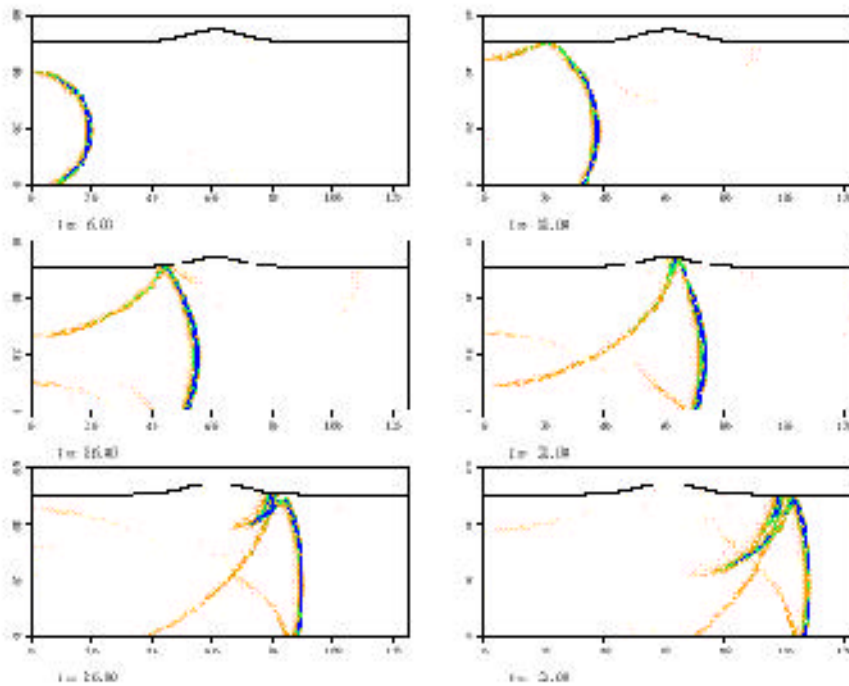


Figure 2: Snap shots of the wave field. the model is a homogeneous half-space with a Gaussian hill on the free surface.

The wavenumber integral can also be done by a FFT.

**Narrow-angle approximation** When small-angle waves prevail such as in the case of Lg propagation, the spectral interpolation in equation (16), which is tricky and even unstable in some cases, can be avoided and replaced by operations in the space domain using a narrow-angle wave approximation.

From (16), it can be seen that to calculate the reflection response we need to find the spectral components  $u_t^+(-\tilde{K}_T)$ . We will try to obtain the approximate space-domain operations corresponding to the wavenumber domain interpolation. We know

$$u_t^+(-\tilde{K}_T) = \int_0^\infty dz e^{i(-K_T \cos 2\theta + \gamma \sin 2\theta)z} u_t^+(z) \quad (17)$$

With narrow-angle approximation,  $k$  therefore,

$$u_t^+(-\tilde{K}_T) = \int_0^\infty dz' e^{iK_T z'} \left[ \frac{1}{\cos 2\theta} e^{iK(\tan 2\theta)z'} u_t^+(z'/\cos 2\theta) \right] \quad (18)$$

We see that the corresponding operations for wavenumber-domain interpolation in the space-domain are a modulation plus a coordinate stretching.

### NON-CONFORMAL COORDINATE TRANSFORM FOR GSP

A non-conformal coordinate transform and the correspondent inverse transform are

$$\begin{cases} x = x \\ \zeta = z - h(x) \end{cases} \quad \text{and} \quad \begin{cases} x = x \\ z = \zeta + h(x) \end{cases} \quad (19)$$

where  $h(x)$  is the height function of free surface topography. Denote the field and the medium parameters in the new coordinate system as  $\hat{u}(x, \zeta)$ ,  $\hat{\mu}(x, \zeta)$  and  $\hat{\rho}(x, \zeta)$  respectively. Assuming that  $\mu$  varies smoothly with  $x$ , the wave equation for SH wave in the new coordinate system can be obtained as

$$(\nabla^2 + k_0^2) \hat{u}(x, \zeta) = -k_0^2 \left\{ \hat{F}_m(x, \zeta) + \hat{F}_s(x, \zeta) \right\} \hat{u}(x, \zeta) \quad (20)$$

where

$k_0 = k_0(x, \zeta)$  and the operators  $\nabla^2 = \partial^2/\partial x^2 + \partial^2/\partial \zeta^2$  is the Laplacian,

$$\hat{F}_m(x, \zeta) = \hat{\varepsilon}_\rho(x, \zeta) + \frac{1}{k_0^2} \nabla \cdot \hat{\varepsilon}_\mu \nabla \quad (21)$$

is the equivalent force term due to the medium heterogeneities, and

$$\hat{F}_s(x, \zeta) = -\frac{1}{k_0^2} \frac{\hat{\mu}}{\mu_0} \left[ h''(x) \frac{\partial}{\partial \zeta} + 2h'(x) \frac{\partial^2}{\partial x \partial \zeta} - (h'(x))^2 \frac{\partial^2}{\partial \zeta^2} \right]$$

is equivalent force term due to the surface topography.

Using local Born approximation, the scattered field generated by the heterogeneities and topographic change of the thin-slab for each step can be written as

$$U(x_1, k_\zeta) = \frac{ik_0^2}{2\gamma} \int_{x'}^{x_1} dx \int_0^\infty d\zeta e^{i\gamma(x_1-x)} 2\cos(k_\zeta \zeta) \left[ \hat{F}_m(x, \zeta) + \hat{F}_s(x, \zeta) \right] \hat{u}_0(x, \zeta) \quad (22)$$

where  $\hat{u}_0(x, \zeta)$  is the local incident field at the slab entrance.

**Scattering due to coordinate transformation.** Assume that the medium in coordinate  $(x, z)$  is homogeneous, that is  $\hat{F}_m(x, \zeta) = (F_m(x, z) = 0$ . The scattered field under the new coordinate system  $(x, \zeta)$  is only due to the coordinate transformation.

$$U(x_1, k_\zeta) = \frac{1}{2\gamma} \int_{x'}^{x_1} dx e^{i\gamma(x_1-x)} C \left[ 2h'(x)A - (h'(x))^2 B + h''(x)D \right] \quad (23)$$

where

$$A = \frac{\partial^2 u_0(x, \zeta)}{\partial \zeta \partial x} = -iS^{-1} \left[ k'_\zeta \gamma' e^{i\gamma'(x-x')} \hat{u}_0(x', k'_\zeta) \right] \quad (24)$$

$$B = \frac{\partial^2 u_0(x, \zeta)}{\partial \zeta^2} = -C^{-1} \left[ k'^2_\zeta e^{i\gamma'(x-x')} \hat{u}_0(x', k'_\zeta) \right] \quad (25)$$

$$D = \frac{\partial u_0(x, \zeta)}{\partial \zeta} = -S^{-1} \left[ k'_\zeta e^{i\gamma'(x-x')} \hat{u}_0(x', k'_\zeta) \right] \quad (26)$$

with  $C[\cdot]$  and  $S[\cdot]$  being the cosine and sine transforms,  $C^{-1}[\cdot]$  and  $S^{-1}[\cdot]$  as their inverse transforms, and

$$\begin{aligned} \hat{u}_0(x, \zeta) &= \frac{1}{2\pi} \int_{-\infty}^{\infty} dk'_\zeta e^{ik'_\zeta \zeta} e^{i\gamma'(x-x')} \hat{u}_0(x', k'_\zeta) \\ &= C^{-1} \left[ e^{i\gamma'(x-x')} \hat{u}_0(x', k'_\zeta) \right] \end{aligned} \quad (27)$$

**Narrow-angle approximation.** Under the narrow-angle wave approximation,  $k_\zeta \approx k'_\zeta \ll \gamma \approx \gamma' \approx k_0$ . Also, invoking a small slope (or smooth topography) approximation such that  $h''(x) \ll 2h'(x)$  and  $[h'(x)]^2 \ll 2h'(x)$ , the last two terms in equation (23) can be neglected. We obtain

$$U(x_1, k_\zeta) = Z(x_1) e^{i\gamma \Delta x} \int_0^\infty d\zeta 2\cos(k_\zeta \zeta) \frac{\partial}{\partial \zeta} \hat{u}_0(x', \zeta) \quad (28)$$

where

$$Z(x_1) = \int_{x'}^{x_1} dx h'(x) \quad (29)$$

The total focusscattering can be obtained by summing the background field and the scattered field

$$\begin{aligned} u(x_1, k_\zeta) &= e^{i\gamma \Delta x} \int_0^\infty d\zeta 2\cos(k_\zeta \zeta) \hat{u}_0(x', \zeta) \\ &+ e^{i\gamma \Delta x} Z(x_1) \int_0^\infty d\zeta 2\cos(k_\zeta \zeta) \frac{\partial}{\partial \zeta} \hat{u}_0(x', \zeta) \\ &= e^{i\gamma \Delta x} \int_0^\infty d\zeta 2\cos(k_\zeta \zeta) e^{Z(x_1) \frac{\partial}{\partial \zeta}} \hat{u}_0(x', \zeta) \end{aligned} \quad (30)$$

where  $x = x_1 - x_1$ . In the last equation, the Rytov transformation is applied to make the operator unitary.

### NUMERICAL EXAMPLES

To test the accuracy and ability of the phase screen method as a propagator for crustal wave guide with rough free surfaces, numerical simulations have been conducted for both conformal and non-conformal methods. The first model is a homogeneous half space with a Gaussian hill. The center of the hill is located at the epicenter distance of 62.5 km, the maximum height of the hill is 4 km and the standard deviation of the Gaussian function is 12.9 km. A SH-wave source is located in the depth of 32 km. The S-wave velocity is 3.5 km/s.

Shown in Fig. 2 are snap shots of the wavefield calculated by the conformal screen method. We can clearly see the incident wave and reflected wave from the free surface. After encountered the Gaussian hill on the surface, the incoming wave split into two arrivals on the ground surface. These interactions complicated the wavefield and provided a test for the new method. Shown in Figs. 3a and 3b are synthetic seismograms for the Gaussian hill model using both conformal and non-conformal methods, respectively. Synthetic seismograms calculated with a more accurate boundary integral method (Fu and Wu, 1999) are used as a reference. In both figures, the solid lines are from the screen method and the dashed lines are from boundary integral method. In Fig. 3a, the conformal screen method uses  $dx = 0.25$  km,  $dz = 0.25$  km and  $dt = 0.05$  sec. The comparisons indicate that the screen method gives a satisfactory result for this model. It correctly modeled waveforms between distances 60 and 70 km, where two reflections from the convex free surface interfere with each other and generate complex waveforms. In Fig. 3b, the non-conformal screen

method uses  $dx = 0.125$  km,  $dz = 0.25$  km and  $dt = 0.05$  sec. in the calculation. Generally speaking, the results are consistent with those from the boundary integral method except there are some minor precursors at distances between 50 and 70 km.

Our next model is for Lg wave propagation in a waveguide with a rough free surface. The model has an average crust thickness of 30 km. A random fluctuation is added to the free surface. The randomness has an exponential power spectrum. Its RMS fluctuation is 0.4 km; horizontal correlation length is 40 km and maximum elevation difference is 1.73 km. These parameters represent the topography of a typical mountain area. A SH-source is located in the depth of 10 km. The conformal transform method is used to calculate the Lg propagation. Parameters used in the calculation are  $dx = 0.25$  km,  $dz = 0.25$  km and  $dt = 0.05$  sec. As a comparison, Fig. 4 gives the snap shots for a crustal wave guide without the surface fluctuation. The figure clearly shows the head wave and multiple reflections between the free surface and Moho discontinuity. All wave fronts are relatively sharp and clear. Fig. 5 gives the snap shots for a crust wave guide with the above mentioned surface fluctuation. With the surface fluctuations, the reflections are combined with randomly scattered waves. These scattered waves blurred the entire wavefield and make part of the energy deflected from its original direction cause the additional Lg attenuation.

### **CONCLUSION AND DISCUSSIONS**

This paper is part of the study aimed at development and application of a new wave propagation and modeling method for regional waves in heterogeneous crustal wave guides using one-way wave approximation. In this paper, two forms of boundary conditions based on conformal and non-conformal coordinate transforms have been developed for taking care of irregular free surfaces for generalized screen propagator. The resulting algorithms can give satisfactory results for models with mild to moderate free surface fluctuations. The comparisons between the method developed here and the more accurate boundary integral method indicate that this method can be used to calculate synthetic seismograms of regional waves for more realistic velocity models, longer propagating distances and higher frequencies.

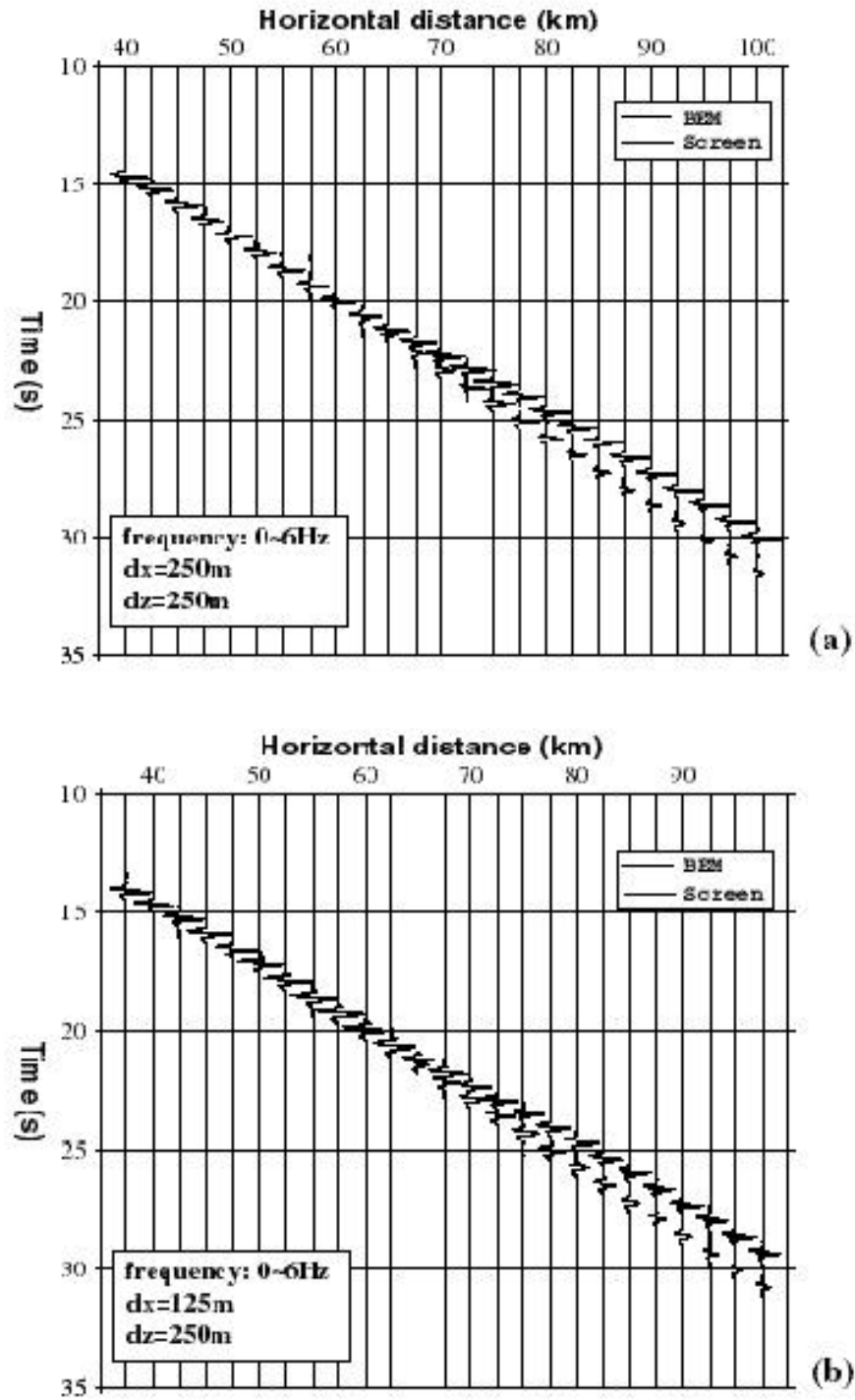


Figure 3: Synthetic seismograms using (a) conformal and (b) non-conformal transform methods, respectively. The solid lines are from the GSP method. The dashed lines are from the boundary integral method, and used as a reference. Details please see the text.

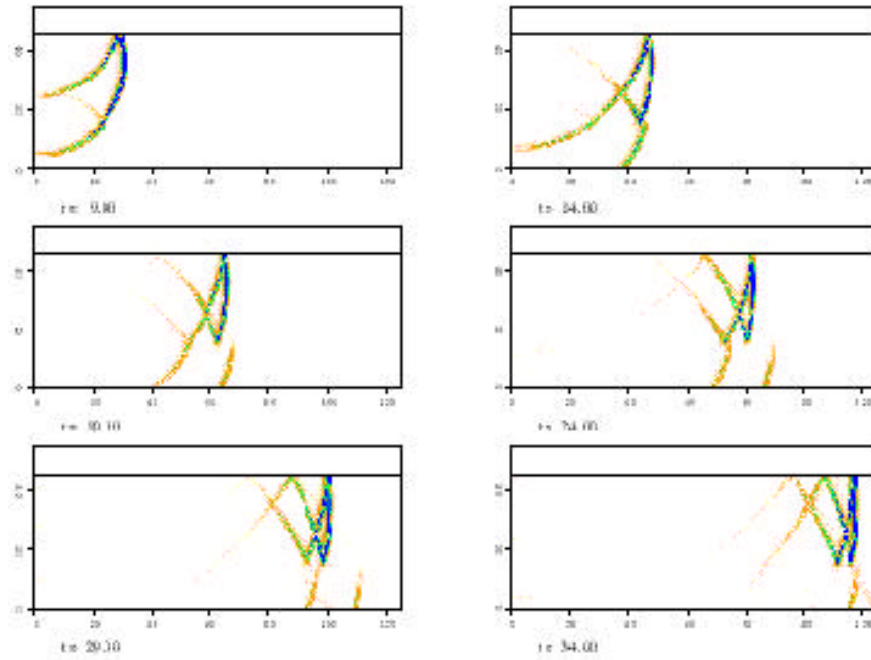


Figure 4: Snap shots of the wave field. the model is a homogeneous crustal wave guide. The depth to the Moho is 30 km. All wave fronts are relatively sharp and clear

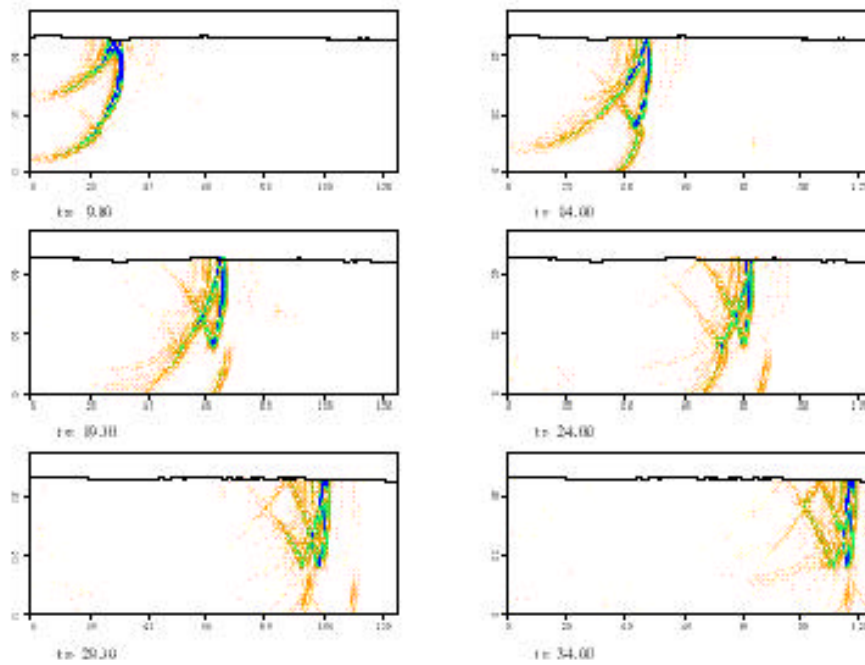


Figure 5: Snap shots of the wave field. the model is a homogeneous crustal wave guide with a rough free surface (for detailed parameters, see the text). With the surface fluctuations, the scattered waves blurred the wavefield.

**REFERENCES**

- Bouchon, M., 1981, A simple method to calculate Green's functions for elastic layered media, *Bull. Seismol. Soc. Am.*, 71, 959-971.
- Bouchon, M., M. Campillo and S. Gaffet, 1989, A boundary integral equation-discrete wavenumber representation method to study wave propagation in multilayered media having irregular interfaces, *Geophysics*, 54, 1134-1140.
- Campillo, M. 1990, Propagation and attenuation characteristics of the crustal phase Lg, *Pure and Appl. Geophys.* 132, 1-19.
- Chen, X.F., 1990, Seismogram synthesis for multi-layered media with irregular interfaces by the global generalized reflection/transmission matrices method - Part I. Theory of 2-D SH case, *Bull. Seismol. Soc. Am.*, 80, 1694-1724.
- Chen, X.F., 1995, Seismogram synthesis for multi-layered media with irregular interfaces by the global generalized reflection/transmission matrices method - Part II. Applications of 2-D SH case, *Bull. Seismol. Soc. Am.*, 85, 1094-1106.
- Fu, L.Y. and R.S. Wu, 1999, A hybrid BE-GS method for modeling regional wave propagation, Submitted to *the CTBT special issue*.
- Jih, R.S., 1996, Waveguide effects of large-scale structural variation, anelastic attenuation and random heterogeneity on SV Lg propagation: a finite-difference modeling study, *Proc. of the 18th Annual SRS on Monitoring a CTBT*, 182-194.
- Kennett, B.L.N., 1984, Guided wave propagation in laterally varying media -I. Theoretical development, *Geophys. J. R. Astr. Soc.* 79, 235-255
- Hestholm, S.O. and B.O. Ruud, 1994, 2-D finite-difference elastic wave modeling including surface topography, *Geophysical Prospecting*, 42, 371-390.
- Hestholm, S.O. and B.O. Ruud, 1998, 3-D finite-difference elastic wave modeling including surface topography, *Geophysics*, 63, 613-622.
- Wu, R. S., 1994, Wide-angle elastic wave one-way propagation in heterogeneous media and an elastic wave complex-screen method, *J. Geophys. Res.*, 99, 751-766.
- Wu, R.S., S. Jin and X.B. Xie, 1999a, Seismic wave propagation and scattering in heterogeneous crustal waveguides using screen propagators: I SH waves, submitted to *Bull. Seism. Soc. Am.*
- Wu, R.S., S. Jin and X.B. Xie, 1999b, Energy partition and attenuation of Lg waves by numerical simulations using screen propagators, submitted to *Phys. Earth and Planet. Inter.*
- Xie, X.B. and T. Lay, 1994, The excitation of explosion Lg, a finite-difference investigation, *Bull. Seismol. Soc. Am.*, 84, 324-342.